Windstorm Hazard Index Development for Malaysia

Nur Hidayah Zakaria[1], Nur Atiqah Hazali[2], Siti Aekbal Salleh[3,4], Nurul Amirah Isa[1], Nini Nurdiana Johari[1], Mohd Badrul Hafiz Che Omar[1], Arnis Asmat[5], Andy Chan[6]

[1] Faculty of Asia Built Environment and Surveying, Universiti Geomatika Malaysia (UGM), Malaysia
[2]Geospatial Science & Technology College (GSTC), Malaysia
[3]Institute for Biodiversity and Sustainable Development (IBSD), Universiti Teknologi MARA, Malaysia.
[4]Faculty of Built Environment, Universiti Teknologi MARA (UiTM) , Malaysia
[5]School of Chemistry & Environment, Faculty of Applied Sciences, Universiti Teknologi MARA (UiTM) Shah Alam, Malaysia
[6]Southampton Solent University, England

Keywords: Windstorm Hazard Index (WHI), Remote Sensing, Geospatial Analysis, AHP–PCA Integration, Disaster Risk Assessment

ABSTRACT:
These Windstorms in Peninsular Malaysia have increased in frequency and severity, posing growing risks to communities, infrastructure, and the national economy. Despite these escalating threats, the region currently lacks a comprehensive, location-specific index capable of evaluating and categorizing windstorm hazards for effective planning and mitigation. This study develops a Windstorm Hazard Index (WHI) to Peninsular Malaysia to assess spatial patterns of windstorm risk and support evidence-based decision-making. Four objectives were addressed: (1) identifying key environmental and geographical factors influencing windstorm occurrences; (2) quantifying these parameters using windstorm records from 2008–2018, numerical simulations generated via WRF-ARW, and urban morphology modelling using Envi-MET; (3) formulating the WHI through the integration of Analytic Hierarchy Process (AHP) and Principal Component Analysis (PCA); and (4) validating the index using documented windstorm events from 2020–2024.The WHI categorizes the peninsula into six hazard levels ranging from very low (0.1–0.5) to extreme (0.901–1.0). Southern and central states, including Negeri Sembilan and Pahang, generally exhibited very low hazard levels, while Kelantan and Terengganu showed moderate risk. High-risk zones were concentrated in northern and coastal regions such as Penang, Kedah, and Perlis, with extreme-risk areas detected in parts of Kedah and Perlis. Results indicate that wind speed, temperature, humidity, precipitation, land use, and urban density strongly influence windstorm intensity, particularly in coastal and densely built environments. Validation confirmed the WHI’s reliability, as extreme-risk classifications aligned with recorded damage patterns. Overall, the WHI serves robust framework for regional hazard assessment and disaster-resilient infrastructure development across Peninsular Malaysia.

1. Introduction

Windstorms are among the most destructive natural hazards, capable of causing severe damage to infrastructure, ecosystems, and human life. In recent years, Peninsular Malaysia has experienced an increase in both the frequency and intensity of windstorm events, reflecting broader trends associated with climate variability and extreme weather conditions (Bachok et al., 2015; Bachok et al., 2018). These events frequently result in structural damage, power outages, and disruptions to transportation systems, particularly in rapidly urbanizing and densely populated regions.

Despite their growing impact, windstorm hazard assessment in Malaysia remains limited due to the absence of a comprehensive, spatially explicit framework. Existing approaches often rely on single-parameter analysis, such as wind speed or rainfall, which fails to capture the complex interactions between meteorological, environmental, and built-environment factors. Previous studies have highlighted the importance of integrating multiple parameters including wind speed, temperature, humidity, precipitation, land use, and topography in hazard modelling (Malczewski, 2006; Feizizadeh et al., 2014). However, their combined effects and relative contributions have not been systematically quantified within the Malaysian context, resulting in limited predictive capability and spatial understanding.

Furthermore, windstorms are characterized by rapid onset and short duration, often lasting less than 30 minutes, which significantly reduces response time and limits the effectiveness of reactive disaster management strategies. This underscores the need for proactive, data-driven tools that can support early warning systems and spatial planning. The lack of a localized hazard index further constrains decision-making, particularly in multi-hazard environments where windstorms may occur alongside floods and modelling (Malczewski, 2006; Feizizadeh et al., 2014). Recent advancements in geospatial modelling and multi-criteria decision-making have enabled more comprehensive approaches to hazard assessment. Techniques such as GIS-based overlay analysis, statistical modelling, and machine learning have been widely applied in natural hazard studies to integrate heterogeneous datasets and generate spatial risk maps (Malczewski, 2006). In particular, the integration of structured decision-making methods with statistical techniques has shown strong potential in improving model robustness by combining expert knowledge with data-driven insights. However, such integrated approaches remain underexplored for windstorm hazard assessment, especially in tropical regions like Malaysia.

The application of the Analytic Hierarchy Process (AHP) allows for systematic weighting of multiple parameters based on their relative importance, while the Principal Component Analysis (PCA) reduces redundancy and identifies dominant influencing factors (Saaty, 1980; Jolliffe, 2002). In addition, numerical weather prediction models such as the WRF-ARW provide high-resolution spatial data on atmospheric conditions, while urban microclimate models such as ENVI-met enable detailed analysis of wind behaviour in built environments (Bruse & Fleer, 1998). The integration of these techniques offers a comprehensive framework for capturing both macro-scale and micro-scale wind dynamics (Samsuddin et al.,2025).

Despite these methodological advancements, there remains a lack of studies that integrate meteorological simulation, urban

https://doi.org/10.5194/isprs-archives-XLIX-B3-2026-1339-2026

morphology, and multi-criteria decision-making into a unified windstorm hazard index. Existing hazard models often lack validation using real-world events, limiting their practical applicability for planning and risk management. Therefore, there is a critical need to develop a validated, spatially explicit index that reflects the complex interactions of environmental and urban factors influencing windstorm hazards.

To address these challenges, this study develops a Windstorm Hazard Index (WHI) tailored to Peninsular Malaysia. The WHI integrates multi-source data, including observational records (2008–2018), numerical simulations, and urban morphology analysis, within a GIS-based framework. The index is further validated using documented windstorm events from 2020–2024 to ensure its reliability and predictive capability.

The main objective of this study is to develop a robust and spatially explicit WHI capable of classifying hazard levels and supporting evidence-based decision-making. The findings contribute to advancing hazard modelling methodologies and provide a practical decision-support tool for urban planners, disaster management agencies, and policymakers in improving resilience to windstorm hazards in Malaysia.

2. Material and Method

2.1 Study Area

Peninsular Malaysia covers approximately 132,000 km² and is located between latitudes 1°N–6°N and longitudes 100°E–104°E. The region is characterized by diverse topography, including coastal lowlands, undulating hills, and the Titiwangsa mountain range, which forms the central backbone of the peninsula. These geographical features contribute to spatial variability in wind patterns and atmospheric conditions.

The regional climate is tropical and strongly influenced by monsoon systems. According to the Malaysian Meteorological Department (Nur Hidayah Zakaria et al., 2019), the northeast monsoon (November–March) is associated with stronger winds and heavy rainfall, particularly along the east coast, while the southwest monsoon (May–September) brings relatively moderate and stable wind conditions (Zakaria et al., 2020). Transitional inter-monsoon periods (April and October) are characterized by light and variable winds, often accompanied by convective thunderstorms. These seasonal variations play a significant role in shaping wind behaviour and the occurrence of windstorm events (Tangang et al., 2012).

Figure 1 shows the study area in Peninsular Malaysia. Climatically, Peninsular Malaysia experiences high annual precipitation ranging from 2,500 to 3,000 mm, with peak rainfall occurring during the monsoon seasons. Temperatures remain relatively uniform throughout the year, averaging between 26°C and 30°C. The average wind speed is generally low, typically between 2 and 4 m/s annually, but can increase significantly during monsoon periods and localized storm events.

Land use across the peninsula is heterogeneous, with forested areas covering approximately 60% of the region, agricultural land about 30%, and urban areas accounting for 7–10%. The remaining areas include water bodies and minimal bare land. Rapid urbanization and agricultural expansion, particularly oil palm cultivation, have contributed to changes in land cover patterns, which may influence wind flow and hazard exposure.

Peninsular Malaysia has experienced multiple windstorm events over the past two decades, particularly during the northeast monsoon season. Notable events in 2011, 2013, and 2018 resulted in significant damage to infrastructure, power disruptions, and localized loss of life. These recurring events highlight the importance of developing a spatially explicit Windstorm Hazard Index (WHI) to assess regional risk patterns and support disaster mitigation and planning efforts.

Figure 1: Study area at Peninsular Malaysia (Retrieve from Jabatan Pemetaan Malaysia (JUPEM) 27 January 2023)

2.2 Data Collection

This study integrates multi-source datasets representing meteorological, environmental, built environment, and social parameters to comprehensively assess windstorm hazards in Peninsular Malaysia. The data were collected from authoritative national and global sources to ensure reliability and consistency. Meteorological data, including wind speed, temperature, relative humidity, precipitation, and atmospheric pressure, were obtained from the Malaysian Meteorological Department (MetMalaysia), Department of Irrigation and Drainage (DID), and Department of Environment (DOE). These datasets provide long-term observations required to capture climatic variability and seasonal wind behaviour. Windstorm event records for the period 2008–2018 were compiled from official reports and secondary sources, including news archives and documented incident databases, to represent historical hazard occurrences.

To enhance spatial representation, numerical simulation data were generated using the WRF-ARW model, which provides high-resolution atmospheric variables across the study area. In addition, urban-scale wind behaviour was analysed using ENVI-met to capture the influence of built environments on wind flow dynamics.

Environmental and topographic data were derived from remote sensing and geospatial sources. Land use/land cover (LULC) data were obtained from satellite imagery (e.g., Landsat 8), while slope information was extracted from digital elevation models (DEM). Built-environment data, including building density and road networks, were sourced from OpenStreetMap (OSM), and population data were obtained from the Department of Statistics Malaysia (DOSM).

All datasets were pre-processed and standardized within a GIS environment to ensure consistency in spatial resolution and format. Rasterization, normalization, and resampling techniques were applied to enable integration of heterogeneous data layers. These datasets form the basis for subsequent analysis, including parameter weighting, dimensionality reduction, and the development of the Windstorm Hazard Index (WHI).

2.3 Method

The methodology of this study consists of four main stages: (1) parameter identification and analysis, (2) wind simulation and urban modelling, (3) development of the Windstorm Hazard Index (WHI), and (4) model validation. The overall workflow integrates multi-source datasets within a GIS-based framework to produce a spatially explicit hazard index.

Relevant parameters influencing windstorm hazards were identified based on literature review and data availability. These include meteorological (wind speed, temperature, humidity, precipitation, pressure), environmental (land use/land cover and slope), built environment (building and road density), and social (population) variables. Statistical analysis, including correlation assessment, was conducted to evaluate the relationships between wind speed and other variables, allowing the selection of significant parameters for further modelling (Zakaria et al,.2023).

2.3.1 AHP and PCA Integration

The development of the Windstorm Hazard Index (WHI) integrates the Analytic Hierarchy Process (AHP) and Principal Component Analysis (PCA) to ensure both expert-driven weighting and data-driven dimensionality reduction. The AHP method was applied to determine the relative importance of selected parameters, including meteorological, environmental, built environment, and social factors. Pairwise comparison matrices were constructed based on expert judgment and supported by literature. The normalized weights were derived, and consistency ratios (CR) were calculated to ensure reliability, with all CR values maintained below the acceptable threshold of 0.1 (Saaty, 1980). AHP has been widely used in hazard assessment due to its ability to structure complex decision problems and incorporate expert knowledge (Malczewski, 2006).

To complement the subjective weighting from AHP, PCA was employed to analyze the variance structure of the dataset and reduce redundancy among correlated variables. Eigenvalue decomposition was used to extract principal components, and only components with eigenvalues greater than 1 were retained (Jolliffe, 2002). PCA has been extensively applied in environmental and hazard modelling to improve data efficiency and reduce multicollinearity (Abdi & Williams, 2010).

The integration of AHP and PCA improves model robustness by combining expert knowledge with statistical evidence, addressing limitations of single method approaches commonly used in hazard modelling (Malczewski, 2006; Jolliffe, 2002).

2.3.2 WHI Development

The Windstorm Hazard Index (WHI) was developed using a GIS-based weighted overlay approach that integrates standardized parameter layers with their respective weights derived from AHP and validated by PCA. All parameters were normalized to a common scale (0–1) to ensure comparability. The WHI was calculated as:

$$\mathrm{WHI}=\sum(W_i \times X_i) \quad (1)$$

where W_i represents the weight of parameter *i*, and X_i represents the standardized value of parameter *i*.

The weighted overlay technique is commonly applied in spatial multi-criteria evaluation for hazard mapping, allowing the integration of multiple datasets within a GIS environment (Malczewski, 2006).

The final WHI map was generated at a spatial resolution of 1 km × 1 km, enabling detailed spatial analysis across Peninsular Malaysia. The index values were classified into six hazard levels: very low (0.1–0.5), low (0.501–0.6), moderate (0.601–0.7), high (0.701–0.8), very high (0.801–0.9), and extreme (0.901–1.0).

2.3.3 Validation

The validation of the Windstorm Hazard Index (WHI) was conducted to assess its predictive accuracy and reliability in identifying windstorm-prone areas. A total of 55 historical windstorm events (2020–2024) were used as validation samples. The validation process involved both spatial analysis in GIS and statistical evaluation. Windstorm event locations were first mapped in ArcGIS Pro, and the WHI raster was overlaid with the event dataset. The WHI values and associated parameter values were extracted at each event location using the *Multi Values to Points* tool, and the resulting dataset was exported for statistical analysis. To evaluate classification performance, confusion matrix-based metrics were applied, including the True Positive Rate (TPR) and False Positive Rate (FPR), defined as:

$$TPR = \frac{TP}{TP + FN'} \ , \ FPR = \frac{FP}{FP + TN} \quad (2)$$

where TPR is the true positive rate, FPR is the false positive rate, TP represents true positives, FP false positives, TN true negatives, and FN false negatives.

The predictive capability of the model was further assessed using the Receiver Operating Characteristic (ROC) curve, which evaluates the trade-off between TPR and FPR across different threshold values (Fawcett, 2006; Hanley & McNeil, 1982). The overall performance was quantified using the Area Under the Curve (AUC):

$$AUC = \int_0^1 TPR\ (FPR)\ d(FPR) \quad (3)$$

where TPR is the true positive rate, FPR is the false positive rate, TP represents true positives, FP false positives, TN true negatives, and FN false negatives. AUC value close to 1.0 indicates excellent predictive performance, while 0.5 indicates random classification.

In addition to classification-based validation, continuous error metrics were employed to evaluate prediction accuracy. The Root Mean Square Error (RMSE) and Mean Absolute Error (MAE) were calculated as:

$$RMSE = \sqrt{\frac{\sum_{i=1}^{n}(P_i - O_i)^2}{n}} \quad (4)$$

$$MAE = \sqrt{\frac{\sum_{i=1}^{n}|P_i - O_i|^2}{n}} \quad (5)$$

Finally, the coefficient of determination (R^2) assessed how well the WHI predictions explained the variance in the observed hazard data:

$$R^2 = \frac{\sum_{i=1}^{n}(O_i - P_i)^2}{\sum_{i=1}^{n}(O_i - \bar{O})^2} \tag{6}$$

where is $\bar{O}$ the mean of observed values. Higher R_2 values indicate stronger agreement between predicted and observed data. To further validate the relationship between WHI classes and observed windstorm occurrences, the Chi-Square Goodness-of-Fit Test was applied:

$$x^2 = \sum \frac{(O_i - E_i)^2}{E_i} \tag{7}$$

Where O_i represents observed frequencies and E_i represents expected frequencies. A statistically significant result ($p < 0.05$) indicates that windstorm occurrences are not randomly distributed but are significantly associated with WHI classifications (McHugh, 2013).
In addition to statistical validation, visual validation was performed using scatterplots and residual analysis to examine the agreement between predicted and observed values. The integration of spatial overlay, statistical metrics, and graphical analysis provides a comprehensive validation framework, ensuring that the WHI is both statistically robust and spatially reliable for windstorm hazard assessment.

3. RESULT AND DISCUSIION

3.1 AHP

The weighting scheme for the Windstorm Hazard Index (WHI) was developed using the Analytic Hierarchy Process (AHP) as shown in table 1, integrating expert judgment and evidence from previous studies to ensure methodological consistency and contextual relevance. The Saaty scale values were assigned based on comparative importance between parameters, where meteorological variables were prioritised due to their direct influence on windstorm formation and intensity.
Wind speed was considered the most critical parameter, as it directly contributes to structural damage and hazard severity, and was therefore assigned higher relative importance compared to precipitation and temperature. Precipitation was also identified as a significant factor influencing storm dynamics, particularly in tropical climates, while temperature and relative humidity were assigned lower values due to their indirect role in atmospheric processes. These parameter relationships are consistent with previous studies on climate-related hazard modelling (Mupepi, 2023; Nguyen et al., 2023).
Environmental and topographic parameters were incorporated to capture terrain and surface interactions. Slope was assigned moderate importance due to its role in influencing wind flow behaviour and terrain-induced acceleration, while land use/land cover (LULC) was considered a key factor affecting surface roughness and damage potential. Infrastructure-related parameters such as building and road were assigned lower weights, as they represent exposure rather than direct hazard drivers. Similarly, population was assigned moderate importance due to its role in representing vulnerability and potential impact, particularly in densely populated areas (Hasan, 2024; Yousefi, 2022).
To reduce subjectivity and improve consistency, the initial Saaty scale values were aggregated using the geometric mean approach. This method is widely applied in group AHP as it preserves reciprocal properties and provides a mathematically robust way to combine multiple judgments into a single representative value (Forman & Peniwati, 1998; Dong et al., 2010). The resulting geometric mean values ranged from 1 to 8, with precipitation (8), pressure (7), and wind speed (5) identified as dominant hazard-driving parameters; while building and road recorded the lowest values (1), indicating their secondary role in hazard generation.
Following aggregation, the pairwise comparison matrix was constructed using ratio-based relationships derived from the Saaty values. The matrix maintained the reciprocal property required in AHP, where each element is the inverse of its corresponding comparison. The presence of fractional values (e.g., 1/7, 1/5, 1/3) reflects the use of aggregated judgments rather than single-expert inputs and allows more precise differentiation between parameters. This approach is methodologically valid, as AHP permits real-number comparisons provided that the consistency of the matrix is maintained (Saaty, 1990).

Table 1: The pairwise comparison matrix presents the relative importance of parameters in Windstorm Hazard Index (WHI) development.

	Building	LULC	Population	Precipitation	Pressure	Relative Humidity	Road	Slope	Temperature	Wind Speed
Building	1	1/3	1/3	1/7	1/7	1/5	1	1/5	1/2	1/6
LULC	3	1	1	1/5	1/5	1/3	3	1/2	1	1/4
Population	3	1	1	1/5	1/5	1/3	3	1/2	1	1/4
Precipitation	7	5	5	1	1	3	7	3	4	5
Pressure	7	5	5	1	1	3	7	3	4	5
Relative Humidity	5	3	3	1/3	1/3	1	3	2	2	3
Road	1	1/3	1/3	1/7	1/7	1/3	1	1/3	1/2	1/4
Slope	5	2	2	1/3	1/3	1/2	3	1	2	3
Temperature	2	1	1	1/4	1/4	1/2	2	1/2	1	1/2
Wind Speed	6	4	4	1/5	1/5	1/3	4	1/3	2	1

The normalized pairwise comparison matrix in Table 2 reveals the relative contribution of each parameter after column standardization. A clear pattern emerges in which precipitation and pressure show consistently high normalized values across most columns. For example, both parameters recorded 0.542 under the LULC and population columns, 0.404 under the road column, 0.344 under the temperature column, and 0.326 under the wind speed column. These values indicate that precipitation and pressure dominated the pairwise comparison structure and exerted strong influence relative to the other criteria. Relative humidity and slope also displayed moderate normalized contributions, while building and road generally remained low across the matrix. This normalized distribution suggests that the hazard-generation component of the model is strongly controlled by meteorological variables, whereas terrain and land-surface variables play supporting roles in shaping where and how those hazards manifest spatially.

Table 2: Normalize Pairwise Comparison Matrix

	Building	LULC	Population	Precipitation	Pressure	Relative Humidity	Road	Slope	Temperature	Wind Speed

Building	0.058	0.036	0.036	0.018	0.018	0.031	0.058	0.026	0.043	0.021
LULC	0.085	0.108	0.108	0.037	0.037	0.063	0.173	0.065	0.086	0.052
Population	0.085	0.108	0.108	0.037	0.037	0.063	0.173	0.065	0.086	0.052
Precipitation	0.198	0.542	0.542	0.186	0.186	0.189	0.404	0.261	0.344	0.326
Pressure	0.198	0.542	0.542	0.186	0.186	0.189	0.404	0.261	0.344	0.326
Relative Humidity	0.142	0.325	0.325	0.062	0.062	0.063	0.173	0.174	0.172	0.195
Road	0.028	0.036	0.036	0.018	0.018	0.021	0.058	0.026	0.043	0.021
Slope	0.142	0.217	0.217	0.062	0.062	0.042	0.173	0.087	0.172	0.195
Temperature	0.057	0.108	0.108	0.047	0.047	0.042	0.116	0.043	0.086	0.065
Wind Speed	0.107	0.145	0.145	0.047	0.047	0.095	0.173	0.087	0.115	0.130

Table 3 presents the final priority weights derived from the normalized matrix, and these weights should be regarded as the definitive AHP outcome for the WHI model. Based on the values reported in the thesis, building recorded the highest priority at 0.200 (20.00%), followed by LULC at 0.195 (19.50%), population at 0.160 (16.00%), precipitation at 0.120 (12.00%), pressure at 0.100 (10.00%), relative humidity at 0.090 (9.00%), road at 0.070 (7.00%), slope at 0.035 (3.50%), temperature at 0.020 (2.00%), and wind speed at 0.010 (1.00%). These results show that the final WHI weighting is dominated by built-environment and exposure-related parameters, particularly building, land use, and population, which together account for 55.50% of the total model weight. In contrast, all meteorological variables combined account for a smaller proportion of the final priority hierarchy.

Table 3: The priority weights for the criteria based on normalize pairwise comparisons.

No	Parameter	Priority	Percentages (%)	Rank
1	Building	0.200	20.00	1
2	LULC	0.195	19.50	2
3	Population	0.160	16.00	3
4	Precipitation	0.120	12.00	4
5	Pressure	0.100	10.00	5
6	Relative Humidity	0.090	9.00	6
7	Road	0.070	7.00	7
8	Slope	0.035	3.50	8
9	Temperature	0.020	2.00	9
10	Wind Speed	0.010	1.00	10

This pattern is highly significant for interpreting the WHI. Although windstorms are physically initiated by atmospheric processes, the AHP results indicate that the model prioritises where impacts are likely to be most severe, rather than focusing only on where storms may form. In practical terms, this means that urban form, population concentration, and land-surface modification are treated as the strongest determinants of mapped windstorm hazard in Peninsular Malaysia. Such a result is defensible because hazard mapping at regional scale often combines hazard intensity with exposure characteristics to identify zones of meaningful risk. Dense building concentration increases the potential for structural damage, urban LULC classes alter surface roughness and airflow, and higher population density reflects greater human exposure. Therefore, the dominance of building, LULC, and population suggests that the WHI is not merely a meteorological index, but a spatial hazard-exposure index. This interpretation aligns with the broader literature on GIS-based multi-criteria disaster mapping, where exposure and vulnerability layers frequently carry major decision weight in final susceptibility maps (Malczewski, 2006; Ishizaka & Labib, 2011).

At the same time, the comparatively low final weight assigned to wind speed (1.00%) requires careful interpretation. This does not mean that wind speed is unimportant in a physical sense. Rather, within the final AHP structure of the thesis, wind speed contributed less to spatial differentiation than building pattern, land use, and population. One possible explanation is that wind speed may vary less spatially at the scale of the peninsula than land-use and settlement variables, while the latter create sharper contrasts in mapped hazard potential. Another explanation is that the AHP framework in this study was designed to support hazard mapping for impact-oriented planning, not solely the climatological modelling of storm genesis. Consequently, the final hierarchy reflects the practical reality that the same meteorological event may cause far greater consequences in densely built and populated areas than in sparsely occupied landscapes. This distinction between storm intensity and hazard consequence is crucial in interpreting the model correctly.

The internal reliability of the AHP result is confirmed by the consistency test reported in Table 4. The analysis involved 45 pairwise comparisons, yielding a principal eigenvalue (λmax) of 11.6203, a consistency index (CI) of 0.18003, and a consistency ratio (CR) of 0.099. According to Saaty’s criterion, a CR of less than 0.10 is considered acceptable, indicating that the judgments are sufficiently coherent for decision-making purposes (Saaty, 1990). The CR value of 0.099 therefore validates the final priority weights and demonstrates that the reconstructed comparison matrix remained logically consistent despite being derived from aggregated values and logarithmic least squares reconstruction. This is an important methodological result because it shows that the integration of literature-based judgments, geometric mean aggregation, and pairwise comparison did not introduce unacceptable inconsistency into the model.

Table 4: AHP Consistency Check Results

	Result	Value
1	Number of comparisons	45
2	Principal Eigenvalue (λ_max)	11.6203
3	Random Index (RI)	1.49
4	Consistency Index (CI)	0.18003
5	Consistency Ratio (CR)	0.099

Overall, the AHP results indicate that the WHI developed in this study is strongly shaped by exposure-oriented spatial variables, particularly building distribution, land use, and population density, while still retaining contributions from key meteorological controls such as precipitation, pressure, and humidity. This confirms that the model is particularly well suited for identifying where windstorm impacts are likely to be concentrated, rather than representing atmospheric forcing alone. The combination of a structured weighting framework, acceptable consistency ratio, and literature-supported pairwise judgments provide a scientifically defensible basis for integrating the selected parameters into the final WHI surface.

3.2 PCA

Principal Component Analysis (PCA) was applied to examine the variance structure of the ten input parameters and to identify which variables contributed most strongly to windstorm hazard variability. The PCA was based on both the correlation and covariance matrices for wind speed, temperature, relative humidity, precipitation, LULC, road, building, slope, population, and pressure. The covariance results indicate that wind speed was positively associated with several urban and atmospheric variables, particularly population (1.376844×10^6) and pressure (7.493265×10^5), while temperature showed a strong positive covariance with building (1.145313×10^5) and population (2.874795×10^6). Relative humidity had strong negative covariance with temperature (-4.680729×10^2) and pressure (-1.458567×10^6), but positive covariance with population (4.277677×10^6) and building (1.551559×10^5). In addition, LULC showed notable covariance with population (8.455361×10^5) and building (3.825054×10^4), while road also showed positive covariance with building (2.957083×10^4) and population (7.020347×10^5). These results confirm that the dataset is not controlled by isolated variables, but by a linked urban environmental system in which atmospheric behaviour and human-modified surfaces interact strongly.

The correlation matrix in the thesis also supports this interpretation. Wind speed showed positive correlation with temperature (28.9919), LULC (16.5056), and pressure (13.3888), while temperature showed strong negative correlation with relative humidity (-9.7106) and LULC (-7.5739). Pressure was negatively related to relative humidity (-4.3283) and LULC (-3.9667), whereas population showed positive association with temperature (7.9636), LULC (3.7392), and pressure (3.6148). Although some of these values are unusually large for a standard Pearson correlation matrix, the pattern reported in the thesis consistently indicates that windstorm-related variability is tightly connected to urbanization, land-surface characteristics, and atmospheric controls. In physical terms, this implies that windstorm susceptibility across Peninsular Malaysia is shaped not only by meteorological forcing, but also by how land use, settlement concentration, and infrastructure modify local exposure and microclimatic conditions. This type of interaction is consistent with PCA being used to reveal dominant covariance structure in multivariate environmental datasets.

Table 5: Covariance Matrix for Principal Component Analysis

	Wind Speed	Temperature	Relative Humidity	Precipitation	LULC	Road	Building	Slope	Population	Pressure
Wind Speed	1.0000	28.9919	1.5276	0.5042	16.5056	1.6686	0.2390	0.4065	0.5823	13.3888
Temperature	28.9919	1.0000	-9.7106	8.6815	-7.5739	2.6707	4.0440	7.1920	7.9636	-1.7120
Relative Humidity	1.5276	-9.7106	1.0000	0.3682	-5.7443	-0.3935	0.1389	0.1840	0.3005	-4.3283
Precipitation	0.5042	8.6815	0.3682	1.0000	4.6415	0.5465	0.2238	0.1686	0.3129	3.9084
LULC	16.5056	-7.5739	-5.7443	4.6415	1.0000	0.8632	2.1561	3.7910	3.7392	-3.9667
Road	1.6686	2.6707	-0.3935	0.5465	0.8632	1.0000	0.2950	0.5461	0.5495	1.0726
Building	0.2390	4.0440	0.1389	0.2238	2.1561	0.2950	1.0000	0.1594	0.1226	1.7671
Slope	0.4065	7.1920	0.1840	0.1686	3.7910	0.5461	0.1594	1.0000	0.2271	3.0360
Population	0.5823	7.9636	0.3005	0.3129	3.7392	0.5495	0.1226	0.2271	1.0000	3.6148
Pressure	13.3888	-1.7120	-4.3283	3.9084	-3.9667	1.0726	1.7671	3.0360	3.6148	1.0000

The eigenvalue results in Table 6 show that the first principal component overwhelmingly dominated the dataset. The eigenvalue for the first component, labelled in the thesis as Wind Speed, was 1.07×10^{11}, whereas the second component, labelled Temperature, had an eigenvalue of 6.91×10^8. All subsequent components were drastically smaller: Relative Humidity = 2054.366, Precipitation = 73.19567, LULC = 28.45139, Road = 10.59104, Building = 3.241357, Slope = 1.720159, and Population = 1.23355. The final component, Pressure, had a negative eigenvalue of -8.8×10^8. This result means that nearly all of the variance in the multivariate dataset was concentrated in the first principal component, with only a small additional amount captured by the second component. The negative eigenvalue reported for the final component should be treated cautiously, because in standard PCA eigenvalues are expected to be non-negative; such a result can indicate numerical instability, multicollinearity, or computational issues in the decomposition procedure.

Table 6 confirms this dominance quantitatively. The first component contributed 100.1757% of the eigenvalue percentage, while the second component contributed 0.6444%, giving a cumulative percentage of 100.82% after the first two components. All remaining components contributed 0%, except the pressure component, which contributed -0.82%. Interpreted strictly according to the thesis, this means that wind speed was the dominant statistical driver of variability in the dataset, while temperature made only a very small secondary contribution. The remaining parameters had negligible statistical contribution after the first two components had been accounted for. In practical terms, the PCA output indicates that if the objective is dimensionality reduction alone, the majority of the dataset's variability can be represented by the first component, with limited improvement from retaining additional components.

The eigenvectors provide a more detailed interpretation of which original variables are associated with each component. For the first component, population had the strongest loading (0.99637), followed by pressure (0.08461), while building had only 0.00985 and wind speed itself had a very small coefficient (0.00001). For the second component, building had the dominant loading (0.98553), while pressure also contributed (0.16781). Other components captured more specialized relationships, such as relative humidity loading strongly on its own component (-0.88220), precipitation loading positively with population (0.88098), LULC loading strongly in the negative direction (-0.98813), road loading strongly negatively (-0.99223), and slope showing a strong negative loading (-0.94047) in its respective component. These eigenvector patterns suggest that, although the eigenvalue structure is dominated by the first two components, different components still isolate specific thematic relationships among land use, infrastructure, topography, and atmospheric variables.

Table 6: Eigenvalue and Eigenvectors for Principal Component Analysis

	Wind Speed	Temperature	Relative Humidity	Precipitation	LULC	Road	Building	Slope	Population	Pressure
Eigenvalues	1.07E+11	6.91E+08	2054.36600	73.19567	28.45139	10.59104	3.24136	1.72016	1.23355	-8.8E+08
Eigenvector	Wind Speed	Temperature	Relative Humidity	Precipitation	LULC	Road	Building	Slope	Population	Pressure
Wind Speed	0.00001	0.00020	0.44804	0.31909	0.79213	-0.00288	-0.05506	-0.20917	-0.15228	-0.00070
Temperature	0.00003	0.00006	0.00587	-0.09047	-0.28095	-0.08588	-0.13822	-0.83443	-0.43599	0.00031
Relative Humidity	0.00004	-0.00028	-0.88220	0.00867	0.44979	-0.00592	-0.02994	-0.12222	-0.05894	0.00206
Precipitation	0.00000	0.00002	0.02034	0.01652	0.02747	-0.01750	0.01070	-0.47118	0.88098	-0.00003
LULC	0.00001	0.00002	0.00190	-0.01057	-0.01689	0.03309	-0.98813	0.12517	0.08028	0.00011
Road	0.00001	0.00003	0.01488	-0.07111	0.04273	-0.99223	-0.02025	0.08539	0.02587	0.00003
Building	0.00985	0.98553	-0.00071	0.00001	0.00000	0.00001	0.00000	0.00000	-0.00001	-0.16922
Slope	0.00001	0.00009	0.14253	-0.94047	0.29738	0.08158	0.00716	-0.00797	0.00235	-0.00018

Population	0.99637	-0.02399	-0.00014	0.00000	0.00000	0.00000	0.00000	0.00000	0.00000	-0.08174
Pressure	0.08461	0.16781	0.00206	0.00007	-0.00023	0.00008	0.00018	0.00033	0.00017	0.98218

Table 7 presents the eigenvalues, percentage of variance, and cumulative variance for ten parameters, namely wind speed, temperature, relative humidity, precipitation, LULC, roads, buildings, slope, population, and pressure. The results indicate that wind speed is the dominant variable, with the highest eigenvalue (1.074×10^{11}), contributing 100.18% of the total variance. This confirms that wind speed is the primary factor influencing the variability of the dataset, consistent with previous studies highlighting wind speed as the key driver in wind-related hazard modelling (Vickery et al., 2006; Xiao et al., 2011). Temperature follows with a significantly smaller eigenvalue (6.91×10^{8}), accounting for only 0.64% of the variance. Together, these two variables explain nearly all the variability in the data. In contrast, the remaining variables including relative humidity, precipitation, LULC, roads, buildings, slope, and population contribute negligibly to the overall variance, with values approaching zero. This suggests that these parameters have limited statistical influence on the dataset once wind speed and temperature are considered, which aligns with findings from multivariate environmental analyses where dominant climatic variables often overshadow secondary factors (Jolliffe, 2002). Based on these findings, only wind speed and temperature were retained for the development of the Windstorm Hazard Index (WHI), as they represent the most significant contributors to data variability. The dominance of wind speed highlights its critical role as the primary hazard-driving factor, while temperature provides a secondary but relevant contribution related to atmospheric conditions. Although other variables may be important for exposure and vulnerability assessments, they do not significantly explain variance in this analysis. This approach ensures that the WHI model remains statistically robust and focused on the most influential parameters, consistent with PCA-based variable selection practices in hazard modelling studies (Jolliffe, 2002).

Table 7: Percent and accumulative eigenvalue for Principal Component Analysis

PC Layer	EigenValue	Percent of EigenValues	Accumulative of EigenValues
Wind Speed	1.07E+11	100.1757	100.1757
Temperature	6.91E+08	0.6444	100.82
Relative Humidity	2054.366	0	100.82
Precipitation	73.19567	0	100.82
LULC	28.45139	0	100.82
Road	10.59104	0	100.82
Building	3.241357	0	100.82
Slope	1.720159	0	100.82
Population	1.23355	0	100.82
Pressure	-8.8E+08	-0.82	100

PCA and AHP do not emphasize the same variables because both methods answer different analytical questions. In the AHP, the highest weights were assigned to building (20.00%), LULC (19.50%), and population (16.00%), reflecting expert judgement on exposure, vulnerability, and impact relevance. In contrast, the PCA results showed that wind speed and temperature contributed most substantially to the total variance, indicating that meteorological factors represent the strongest statistical signals in the dataset.
This difference is not a contradiction. AHP is a decision-based weighting method, while PCA is a data-driven variance-maximization technique. Therefore, PCA supports the dominance of atmospheric drivers, especially wind speed, whereas AHP broadens the WHI by incorporating built environment, land-use, and population factors that are important for spatial hazard assessment and planning.

The final PCA conclusion suggests that only wind speed and temperature should be retained for PCA-based weighting, as they explain almost all observed variance. Thus, PCA functions mainly as a statistical screening tool, while AHP provides contextual relevance for multi-parameter hazard modelling. Together, both approaches strengthen the WHI by combining statistical justification with expert-based hazard interpretation. This is consistent with the use of PCA to distinguish dominant physical drivers and reduce multicollinearity in environmental modelling (Jolliffe, 2002).

3.3 WHI DEVELOPMENT

The Windstorm Hazard Index (WHI) was generated through a GIS-based multi-criteria framework and classified into six hazard levels using the Jenks Natural Breaks method (Table 8). This method ensures optimal separation of data by minimizing within-class variance and maximizing between-class differences, thereby producing statistically meaningful hazard zones (Jenks, 1967; Slocum et al., 2009). The WHI values range from 0.001 to 1.0, representing very low to extreme hazard levels.
The spatial distribution of WHI across Peninsular Malaysia (Figure 2) reveals a clear gradient of hazard intensity. Approximately 30–35% of the study area falls within the very low hazard class (0.001–0.5), predominantly located in the central and southern regions, including Negeri Sembilan, Pahang, and parts of Selangor and Johor. These areas are characterized by relatively stable atmospheric conditions and reduced exposure to strong monsoon-driven winds, resulting in minimal windstorm risk.
The low hazard class (0.501–0.6) accounts for approximately 15–20% of the study area, extending into parts of Perak, Selangor, and southern Johor. These regions exhibit slightly higher susceptibility but remain largely stable compared to higher-risk zones.
Moderate hazard areas (0.601–0.7) represent approximately 15–20% of the total area and are primarily distributed along the east coast, including Kelantan, Terengganu, and parts of Pahang. These regions are influenced by seasonal monsoon systems, which contribute to increased wind variability and storm occurrence.
The high hazard class (0.701–0.8) covers approximately 10–15% of the study area, concentrated mainly in the northwestern and coastal regions, including Perlis, Kedah, Penang, and selected coastal zones of Johor and Melaka. These areas experience stronger wind exposure due to coastal effects and atmospheric instability.
The very high hazard class (0.801–0.9) accounts for approximately 5–10% of the study area, primarily located in northern Peninsular Malaysia, particularly Kedah and Perlis. These regions are highly exposed to northeast monsoon winds and exhibit increased susceptibility to intense windstorm events.
The extreme hazard class (0.901–1.0) represents the smallest proportion, approximately 3–5% of the total area, but is highly concentrated in Perlis and Kedah, forming the most critical windstorm hotspot in the peninsula. These areas experience the highest probability of severe windstorm impacts and require priority attention in disaster risk management.
The observed spatial variation in WHI reflects the combined influence of meteorological, environmental, and socio-economic factors. Meteorological variables such as wind speed, precipitation, and atmospheric pressure are the primary drivers

of hazard intensity, particularly in northern and coastal regions. Environmental factors, including land use/land cover and slope, influence the spatial distribution by modifying wind flow patterns. Meanwhile, socio-economic variables such as population density, building concentration, and road networks increase exposure and vulnerability, particularly in urbanized areas.

Overall, the WHI demonstrates that windstorm hazard in Peninsular Malaysia is highly spatially heterogeneous, with the northern region exhibiting the highest concentration of high to extreme hazard zones, while the central and southern regions remain relatively low risk.

Table 8: Windstorm hazard index threshold

Windstorm Hazard Index		Level of Risk
1	0.001 – 0.5	Very Low
2	0.501 – 0.6	Low
3	0.601 – 0.7	Moderate
4	0.701 – 0.8	High
5	0.801 – 0.9	Very High
6	0.901 – 1.0	Extreme

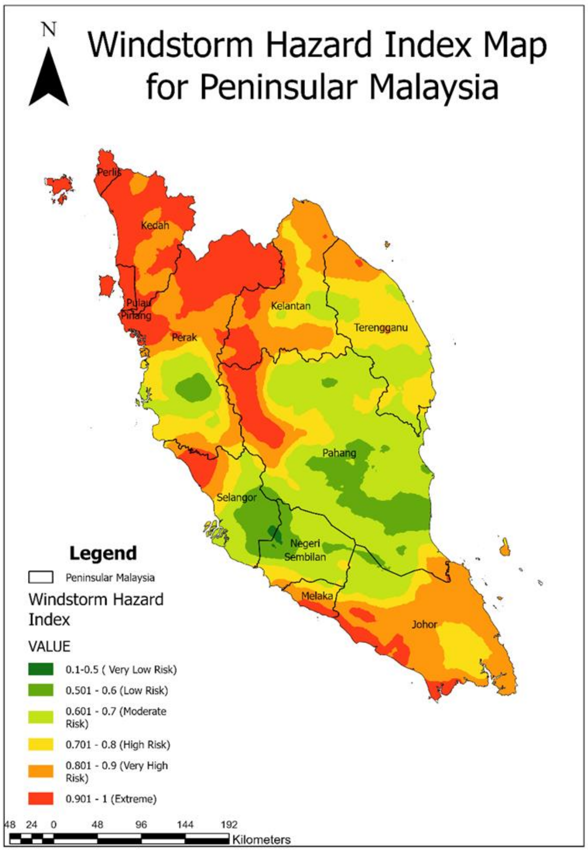

Figure 2: Windstorm Hazard Index Map for Peninsular Malaysia

3.4 WHI VALIDATION

The predictive performance of the Windstorm Hazard Index (WHI) was evaluated using both real windstorm cases and statistical validation methods. A total of 55 documented windstorm events recorded between 2020 and 2024 were used to assess whether the spatial distribution of observed cases corresponded with the hazard classes derived from the WHI map as shown in figure 3. In addition, the statistical robustness of the index was examined using the Receiver Operating Characteristic (ROC) analysis and the Chi-Square Goodness-of-Fit Test, which are widely applied techniques in hazard model validation (Fawcett, 2006; McHugh, 2013).

The distribution of observed windstorm events across WHI classes shows a clear concentration in the higher-risk categories (Table 9). The Extreme class recorded the highest number of events (19 cases), followed by the Moderate class (13 cases) and the Very High class (10 cases). The Low (7 cases) and High (6 cases) classes recorded comparatively fewer events. This distribution indicates that areas classified with higher WHI values generally correspond to a greater number of recorded windstorm occurrences, supporting the practical validity of the index. Although the High class recorded fewer cases than expected, this may reflect localized effects of topography, seasonal atmospheric variability, or site-specific meteorological conditions that are not fully captured by class frequency alone, as commonly observed in spatial hazard modelling studies (Malczewski, 2006).

Table 9: Total count from Windstorm Hazard event in Peninsular Malaysia

No	WHI Level	Event Count
1	Extreme	19
2	Moderate	13
3	Very High	10
4	Low	7
5	High	6

The spatial overlay between the WHI map and the validation dataset further confirms the reliability of the model. As shown in Figure 3, many observed windstorm events are clustered within very high and extreme hazard zones, particularly in Johor, Kedah, Penang, and parts of Selangor. For example, several locations in Johor, including Taman Johor Jaya and Kangkar, were classified as Extreme with WHI values of 0.82, while Kg Skudai Kiri recorded a Very High WHI value of 0.91. In Kedah, cases such as Kg Yooi, Langkawi (0.94) and Pendang (0.96) also fall within the Extreme category, while Kulim (0.90) and Langkawi (0.93) were classified as Very High and High, respectively. Similarly, in Terengganu, Hulu Terengganu recorded Very High WHI values (0.71), while Dungun was classified as Extreme. These patterns demonstrate that the WHI successfully identifies areas where windstorm impacts have historically occurred.

The validation dataset also provides insight into the environmental and socio-spatial conditions of affected areas. Locations with higher WHI values were commonly associated with dense population, greater building concentration, and sub-urban or urban land use classes, suggesting that exposure-related variables played a major role in the resulting hazard pattern. This is especially evident in Johor, Kuala Lumpur, and Kedah, where multiple events occurred in built-up areas with relatively high population counts and building density. These observations are consistent with previous studies indicating that urbanization and land-use modification increase vulnerability to extreme weather events (Wang et al., 2018).

The ROC analysis shows that the WHI has strong predictive capability. The model achieved an Area Under the Curve (AUC) value of 0.86, indicating very good classification performance in distinguishing between windstorm-prone and non-prone areas (Fawcett, 2006). Since an AUC value between 0.8 and 0.9 is generally interpreted as strong predictive performance, this result confirms that the WHI is effective in identifying spatial patterns of windstorm susceptibility. The ROC curve also remained well above the diagonal reference line, demonstrating that the model performs substantially better han random classification.

To further test whether windstorm occurrences were significantly associated with WHI classes, a Chi-Square Goodness-of-Fit Test was performed. The results (Table 10) produced a Chi-Square value of 14.46, with 5 degrees of freedom and a p-value of 0.0129. Since $p < 0.05$, the null hypothesis of random distribution is rejected, indicating that the observed windstorm events are significantly associated with the WHI classification scheme. This result confirms that the WHI does not assign hazard classes arbitrarily, but rather captures meaningful differences in windstorm susceptibility across Peninsular Malaysia, consistent with standard statistical interpretation (McHugh, 2013).

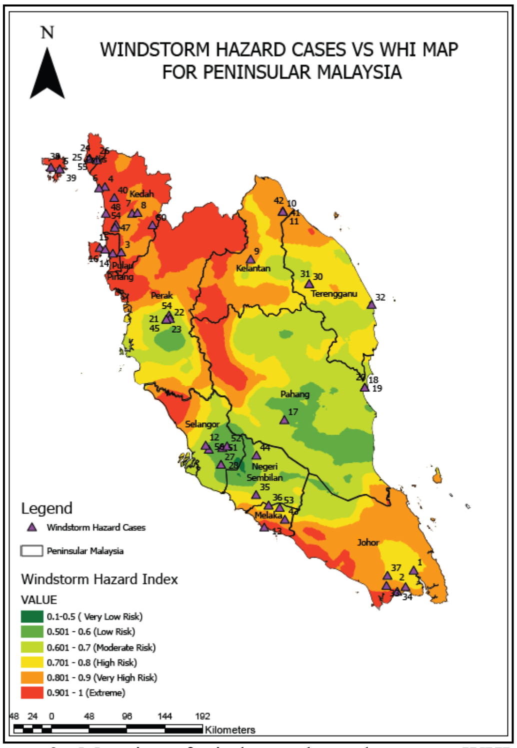

Figure 3: Mapping of windstorm hazard cases on WHI map.

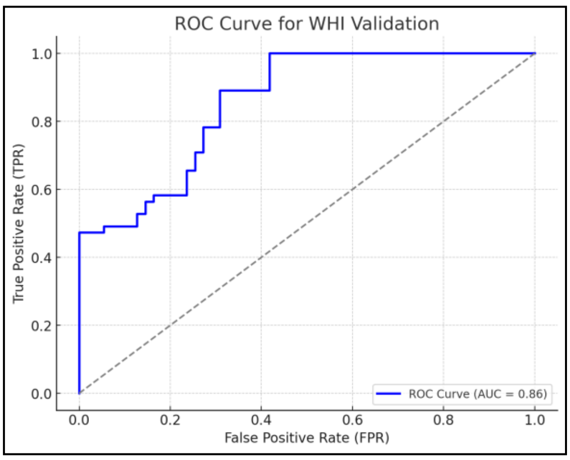

Figure 4: ROC curve analysis TPR and FPR

Table 10: Statistical validation of WHI distribution using Chi - Square

No.	Statistic	Value
1	Chi-Square Value	14.46
2	Degrees of Freedom	5.0
3	P-Value	0.0129

Overall, the validation results demonstrate that the WHI is both spatially reliable and statistically robust. The combination of map-based validation, event frequency analysis, ROC performance, and Chi-Square significance indicates that the index is capable of representing actual windstorm hazard patterns in Peninsular Malaysia. This supports its application as a practical tool for hazard mapping, disaster preparedness, and risk-informed planning, particularly in urbanized and coastal regions where windstorm impacts are more concentrated.

4. CONCLUSION

This study developed and validated a Windstorm Hazard Index (WHI) for Peninsular Malaysia by integrating multi-source environmental, meteorological, and socio-spatial parameters within a GIS-based framework. The combined application of the Analytic Hierarchy Process (AHP) and Principal Component Analysis (PCA) enabled a balanced approach, where AHP captured exposure-driven spatial relevance highlighting building (20.00%), LULC (19.50%), and population (16.00%) as dominant factors while PCA identified wind speed as the primary statistical driver of variance. The resulting WHI map revealed a clear spatial gradient, with high to extreme hazard zones concentrated in the northern and coastal regions, particularly Kedah and Perlis, while central and southern regions exhibited predominantly low hazard levels. Validation using 55 recorded windstorm events (2020–2024) demonstrated strong spatial agreement between observed cases and high-risk WHI zones, supported by robust statistical performance, including an AUC value of 0.86 and a significant Chi-square result ($\chi^2 = 14.46$, $p = 0.0129$). These findings confirm that the WHI is both statistically reliable and spatially meaningful, effectively capturing the interaction between atmospheric drivers and exposure-related factors. Overall, the WHI provides a practical and scientifically grounded tool for windstorm hazard assessment, offering valuable support for disaster risk reduction, urban planning, and climate resilience strategies in Malaysia.

ACKNOWLEDGMENT

The authors gratefully acknowledge the support of the International Society for Photogrammetry and Remote Sensing (ISPRS) through the CP Lo Award Travel Grant, which facilitated participation in the ISPRS Congress 2026. The authors also extend their appreciation to Universiti Geomatika Malaysia and for their academic support and valuable contributions to this research. Also to Univesiti Teknologi MARA for grant FRGS/1/2019/WAB03/UITM/02/1.

References

Abdi, H., & Williams, L. J. (2010). Principal component analysis. Wiley Interdisciplinary Reviews: Computational Statistics, 2(4), 433–459. https://doi.org/10.1002/wics.101

Bachok, M. F., Shamsudin, S., & Zainal Abidin, R. (2015). Effectiveness of windstorm-producing thunderstorms early warning issues in Peninsular Malaysia. International Journal of Environmental Science and Development, 6(9), 635–642. https://doi.org/10.7763/IJESD.2015.V6.672

Bachok, M. F., Shamsudin, S., & Zainal Abidin, R. (2018). Establishment of windstorm-producing thunderstorms hazard threshold in Peninsular Malaysia. ARPN Journal of Engineering and Applied Sciences, 13(17), 7364–7372.

Bruse, M., & Fleer, H. (1998). Simulating surface–plant–air interactions inside urban environments with a three dimensional numerical model. Environmental Modelling & Software, 13(3–4), 373–384. https://doi.org/10.1016/S1364-8152(98)00042-5

Dong, Y., Zhang, G., Hong, W. C., & Xu, Y. (2010). Consensus models for AHP group decision making under row geometric mean prioritization method. Decision Support Systems, 49(3), 281–289. https://doi.org/10.1016/j.dss.2010.03.003

Fawcett, T. (2006). An introduction to ROC analysis. Pattern Recognition Letters, 27(8), 861–874. https://doi.org/10.1016/j.patrec.2005.10.010

Feizizadeh, B., Blaschke, T., & Jankowski, P. (2014). A GIS based spatially-explicit sensitivity and uncertainty analysis approach for multi-criteria decision analysis. Computers & Geosciences, 64, 81–95. https://doi.org/10.1016/j.cageo.2013.11.009

Forman, E., & Gass, S. I. (2001). The analytic hierarchy process—An exposition. Operations Research, 49(4), 469–486. https://doi.org/10.1287/opre.49.4.469.11231

Forman, E., & Peniwati, K. (1998). Aggregating individual judgments and priorities with the analytic hierarchy process. European Journal of Operational Research, 108(1), 165–169. https://doi.org/10.1016/S0377-2217(97)00244-0

Hanley, J. A., & McNeil, B. J. (1982). The meaning and use of the area under a receiver operating characteristic (ROC) curve. Radiology, 143(1), 29–36. https://doi.org/10.1148/radiology.143.1.7063747

Hasan, I. (2024). Geo-spatial based cyclone shelter suitability assessment using analytical hierarchy process (AHP) in the coastal region of Bangladesh.

Ishizaka, A., & Labib, A. (2011). Review of the main developments in the analytic hierarchy process. Expert Systems with Applications, 38(11), 14336–14345. https://doi.org/10.1016/j.eswa.2011.04.143

Jenks, G. F. (1967). The data model concept in statistical mapping. International Yearbook of Cartography, 7, 186–190.

Jolliffe, I. T. (2002). Principal component analysis (2nd ed.). Springer. https://doi.org/10.1007/b98835

Malczewski, J. (2006). GIS-based multicriteria decision analysis: A survey of the literature. International Journal of Geographical Information Science, 20(7), 703–726. https://doi.org/10.1080/13658810600661508

McHugh, M. L. (2013). The chi-square test of independence. Biochemia Medica, 23(2), 143–149. https://doi.org/10.11613/BM.2013.018

Mupepi, O. (2023). A geographic information system and analytic hierarchy process drought risk analysis approach in arid south-western Zimbabwe: Prospects for informed resilience building.

Nguyen, T. T., Nguyen, H. T., & Pham, T. T. H. (2023). Climate change vulnerability assessment using GIS and fuzzy AHP.

Nur Hidayah Zakaria, Salleh, S. A., Asmat, A., & Islam, M. A. (2019). Seasonal windstorm pattern and damages in Peninsular Malaysia 2018. IOP Conference Series: Earth and Environmental Science, 385(1), 012029. https://doi.org/10.1088/1755-1315/385/1/012029

Saaty, T. L. (1990). How to make a decision: The analytic hierarchy process. European Journal of Operational Research, 48(1), 9–26. https://doi.org/10.1016/0377-2217(90)90057-I

Samsuddin, N., Salleh, S. A., Khalid, N., Mohamed Saraf, N., Yaman, R., Pintor, L., Rueda, G., & Samsuddin, N. (2025). Assessing the Heat Vulnerability Index (HVI) in Klang Valley Using Principal Component Analysis (PCA) and an Equal-Weighted Approach. Forum Geografi, 39(2), 188–208. https://doi.org/10.23917/forgeo.v39i2.8633

Slocum, T. A., McMaster, R. B., Kessler, F. C., & Howard, H. H. (2009). Thematic cartography and geovisualization (3rd ed.). Pearson.

Tangang, F. T., Juneng, L., Salimun, E., Sei, K. M., Le, L. J., Muhamad, H., & Ting, M. F. (2012). Climate change and variability over Malaysia: Gaps in science and research information. Sains Malaysiana, 41(11), 1355–1366.

Vickery, P. J., Skerlj, P. F., Lin, J., Twisdale, L. A., Young, M. A., & Lavelle, F. M. (2006). HAZUS-MH hurricane model methodology. I: Hurricane hazard, terrain, and wind load modeling. Natural Hazards Review, 7(2), 82–93. https://doi.org/10.1061/(ASCE)1527-6988(2006)7:2(82)

Wang, J., Yang, Y., & Wang, Y. (2018). Urbanization and its impact on extreme weather events. Science of the Total Environment, 607–608, 131–140. https://doi.org/10.1016/j.scitotenv.2017.06.204

Xiao, Y. F., Duan, Z. D., Xiao, Y. Q., Ou, J. P., Chang, L., & Li, Q. S. (2011). Typhoon wind hazard analysis for southeast China coastal regions. Structural Safety, 33(4–5), 286–295. https://doi.org/10.1016/j.strusafe.2011.04.003

Yousefi, H. (2022). Multi-criteria decision-making system for wind farm site selection using geographic information system (GIS): Case study of Semnan Province, Iran.

Zakaria, N. H., Salleh, S. A., Asmat, A., Chan, A., Isa, N. A., Hazali, N. A., & Islam, M. A. (2020). Analysis of Wind Speed, Humidity and Temperature: Variability and Trend in 2017. IOP Conference Series: Earth and Environmental Science, 489(1), 012013. https://doi.org/10.1088/1755-1315/489/1/012013

Zakaria, N. H., Salleh, S. A., Chan, A., Ooi, M. C. G., Isa, N. A., & Latif, Z. A. (2023). Windstorm Hazardous Area Mapping Using Multi-Criteria Evaluation Techniques of Fuzzy Logic Approach. IOP Conference Series: Earth and Environmental Science, 1217(1), 012036.